Available online at www.sciencedirect.com
ScienceDirect
PHOTONICS AND NANOSTRUCTURES Fundamentals and Applications
Photonics and Nanostructures – Fundamentals and Applications 8 (2010) 264–272
www.elsevier.com/locate/photonics

Invited paper

Stored light in a plasmonic nanocavity based on extremely-small-energy-velocity modes

Dmitry Yu. Fedyanin *, Aleksey V. Arsenin

Department of General Physics, Moscow Institute of Physics and Technology (State University), 9, Institutsky Lane, Dolgoprudny 141700, Russia

Received 17 January 2010; received in revised form 26 April 2010; accepted 28 April 2010
Available online 5 May 2010

Abstract

We propose a novel scheme of the plasmonic cavity that is based on the insulator–metal–insulator (IMI) waveguide of finite length. Surface plasmon polaritons (SPPs) guided by the IMI structure can exhibit extremely small energy velocity if the metal film is thin enough. In that case, the losses are determined mainly by the intrinsic properties of the metal rather than the geometry of the cavity. Accordingly, we should care only about the purity of the metal and need not accurately control the length of the cavity that simplifies the fabrication process. All dimensions of the cavity can be less than the wavelength of light, therefore it is a really nanoscale device. In this paper, we characterize the cavity analytically and demonstrate the stored light using our finite difference time domain (FDTD) code.

Keywords: Thin films; Plasmonic waveguide; Zero energy velocity; Slow light; Cavity; Stored light

1. Introduction

Extremely high velocity of light makes it ideal for communications at a long distance but unsuitable for information handling, however, an ability to control the velocity of ultra-short light pulses opens the door to optical data processing and creation of all-optical routers and memories. Slow light provides the way to compact delay lines and strong light–matter interaction that is necessary for detection of light signals, non-linear and quantum operations and optical data storage. Metamaterial waveguides may give us an ability to slow down and stop light [1,2], but their fabrication requires the size of metallic and dielectric inclusions to be much smaller than the wavelength of the electromagnetic radiation that makes them ideal for GHz and THz devices and limits their applicability in integrated circuits at optical wavelengths. Photonic crystals are almost excellent [3], but the typical dimension of modern electronic integrated circuits is less than 50 nm as compared to the typical dimension of optical elements of 1 μm, which is 20 times larger. Plasmonics is the most promising way to overcome this problem [4–6]. SPPs, electromagnetic waves propagating at the interface between a metal and an insulator, allow to get over the usual diffraction limit [7–10]. An exceedingly short wavelength and a very high spatial localization of the electromagnetic field near the interface yield to the dimension of the order of 100 nm that is comparable with electronic components [4].

The straight way to slow down light and almost completely stop it is to realize zero group velocity (ZGV) dispersion. ZGV as a result of the interference of forward and backward waves can be easily achieved by structuring that takes place in plasmon gratings [7,8] and plasmonic crystals [11], however a periodicity is not the only way to obtain ZGV dispersion. Planar IMI waveguides can exhibit ZGV modes by themselves rather than space harmonics of periodic structures

* Corresponding author. Tel.: +7 926 0806104.
E-mail address: feddu@mail.ru (D.Yu. Fedyanin).

1569-4410/$ – see front matter
doi:10.1016/j.photonics.2010.04.012

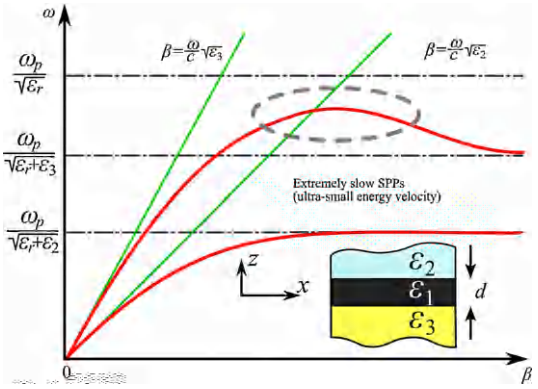

Fig. 1. Dispersion curves of the SPP guided by the IMI guide in the lossless case, β is the propagation constant, ω is the angular frequency. The lower line corresponds to the symmetric mode (the amplitude of the longitudinal electric field does not exhibit a zero inside the metal film) and the upper line to the antisymmetric one. An illustration of the IMI guide is shown in the inset. The core is the metal with dielectric function $\varepsilon_1(\omega)$, the claddings are insulators with different permittivities ε_2 and ε_3 ($\varepsilon_2 > \varepsilon_3$).

[12–15] (Fig. 1). The size of the device based on a periodic structure cannot be less than several periods, while in the case of the ZGV mode the transverse size is limited only by the SPP wavelength (λ_{spp}).

Previously [15,16], IMI and IIM (insulator–insulator–metal) guides were considered in the case of small losses and it was proposed that ZGV modes could be used to design a cavity with a high quality factor, but a strong absorption in the metal modifies SPP dispersion curves and prevents us to achieve ZGV [17–19]. Moreover, the propagation length of slow SPPs (L_{spp}) is less than λ_{spp}. Such a barrier seems to be insurmountable. However, here we demonstrate a cavity with a high Q-factor, based on extremely slow SPPs.

2. Theoretical background

The IMI waveguide under consideration is sketched in the inset of Fig. 1. This guide provides the field confinement along the z-direction and the guide axis coincides with the x-axis. Dispersion relation of the SPP guided by a thin film of thickness d, which is surrounded by two half-spaces with different dielectric functions, is well known [7,8,14] and there is no need to discuss it again. In the current paper, we concentrate our attention on the Al_2O_3–Ag-ZrO_2 guide, though one can consider another IMI structure and obtain similar results. Also, we assume the metal to be described by the general Drude model ($\varepsilon_1 = \varepsilon_r - \omega_p^2/(\omega^2 + i\Gamma\omega)$), where ε_r is the high frequency dielectric constant, ω_p is the plasma frequency and Γ is the damping constant) and thus determine the silver dielectric function as $\varepsilon_1(\omega) = 5.6 - (1.48 \times 10^{16})^2/\omega^2 + i\Gamma\omega)$ in the wavelength range 340–550 nm according to the experimental data in Ref. [20].

Applying the variation theorem [12,21] to the lossless waveguide ($\Gamma = 0$), we get that $\upsilon_E = \upsilon_g$, where:

$$\upsilon_E = \int_{-\infty}^{+\infty} Re(S_x)\mathrm{d}z \Big/ \int_{-\infty}^{+\infty} W\mathrm{d}z = I \Big/ \int_{-\infty}^{+\infty} W\mathrm{d}z \qquad (1)$$

is the energy velocity, the velocity of energy transfer [22,23], (W is the time-average energy density, I is the time-average total power flow and S_x is the x-component of the complex Poynting vector) and:

$$\upsilon_g = \frac{\partial\omega}{\partial\beta} \qquad (2)$$

is the group velocity. In other words, the group velocity and the energy velocity are indistinguishable

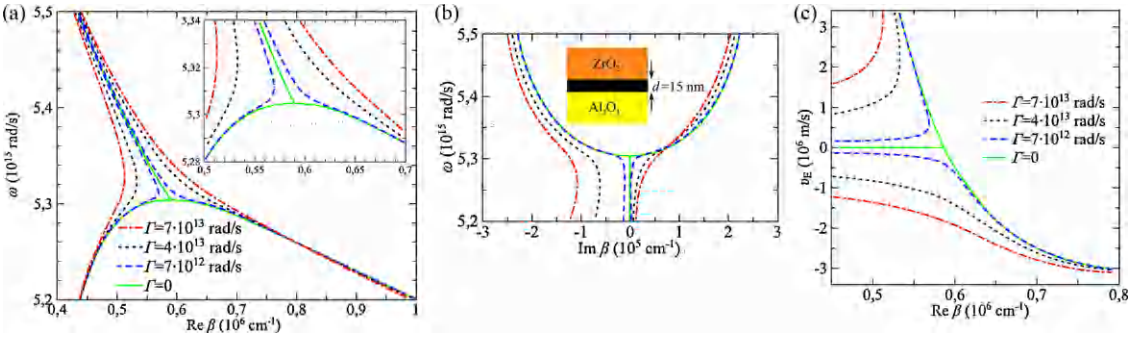

Fig. 2. (a and b) Dispersion curves of the SPP in the Al_2O_3–Ag-ZrO_2 waveguide structure using the complex-β approach (only the antisymmetric mode is shown) for different values of the damping constant ($\Gamma = 7 \times 10^{13}$ rad s^{-1} (dash-dotted red line), $\Gamma = 4 \times 10^{13}$ rad s^{-1} (dotted black line), $\Gamma = 7 \times 10^{12}$ rad s^{-1} (dashed blue line) and $\Gamma = 0$ (solid green line)): angular frequency dependences on the real (a) and imaginary (b) parts of the wavevector β. Energy velocity of the SPP versus the real part of the wavevector (c). Permittivities of Al_2O_3 and ZrO_2 equal 2.84 and 5.5, respectively, and $d = 15$ nm. (For interpretation of the references to color in this figure legend, the reader is referred to the web version of the article.)

in the lossless case that is not valid for lossy guides [22]: $\upsilon_E \neq \upsilon_g$, as follows from the variation theorem. It was shown that the dispersion curves in the lossy and lossless cases differ appreciably only on the vicinity of the point of ZGV [19], so are energy velocities (Fig. 2(a) and (b)). In this region, the imaginary part of the SPP wavevector is large enough and the group velocity given by Eq. (2) does not have a clear meaning as a transport velocity, despite the fact that it can be meaningfully defined even in the case of high losses and dispersion [23], while the energy velocity still determines the velocity of energy transfer [24,25]. We are interested in extremely slow SPPs, therefore we deal with the energy velocity instead of the group velocity. Nevertheless, the term ZGV will be used hereinafter but it will relate only to the lossless waveguide ($\Gamma = 0$) and so it is the same as the zero energy velocity in that case.

An explicit expression for the energy velocity of the SPP in the IMI guide can be derived [19]:

$$\int_{-\infty}^{+\infty} S_x(x,z,t)\mathrm{d}z = \frac{c}{16\pi}\frac{\beta}{k}|H_{\mathrm{low}}(x,t)|^2 \times \left\{\frac{1}{\varepsilon_3 \mathrm{Re}\kappa_3} + \frac{\varepsilon_2}{\varepsilon_3^2 \mathrm{Re}\kappa_2}\frac{|\gamma_{3+}|^2}{|\gamma_{2-}|^2} + \frac{|\gamma_{3+}|^2 + |\gamma_{3-}|^2}{2|\kappa_1|^2\varepsilon_3^2} \times \frac{\sinh(\mathrm{Re}\kappa_1 d)}{\mathrm{Re}\kappa_1} + \frac{\gamma_{3+}\gamma_{3-}^* + \gamma_{3+}^*\gamma_{3-}}{2|\kappa_1|^2\varepsilon_3^2}\frac{\sin(\mathrm{Im}\kappa_1 d)}{\mathrm{Im}\kappa_1}\right\}, \quad (3)$$

Is it possible to decrease the energy velocity down to zero? Unfortunately, no. Losses due to strong absorption in the metal prevent us from doing so. Then, how slow SPP can be achieved? It turns out, that the energy velocity can be sufficiently small ($\approx 5 \times 10^{-3}\, c$) (Fig. 2(c)) for the thin silver film guide at room temperature ($\Gamma = 7 \times 10^{13}$ rad s^{-1}) and still less ($\approx 5 \times 10^{-4}\, c$) for ten times lower value of the damping constant ($\Gamma = 7 \times 10^{12}$ rad s^{-1}). Thus, the energy velocity can be extremely small in spite of high absorption. What is wrong with extremely slow SPPs? The propagation length is too small [17,19]. The figure of merit does not exceed ten for the Al_2O_3–Ag-ZrO_2 guide at room temperature and, if the energy velocity is close to its minimum absolute value, the figure of merit is less than 5 (Fig. 3). If we increase the figure of merit by changing the operating frequency, we increase the energy velocity significantly. Therefore, if one deals with ultra-slow SPPs, one deals with low figures of merit. For instance, at the frequency of ZGV (Fig. 2, $\omega = 5.305 \times 10^{15}$ rad s^{-1}) the figure of merit equals 5.0 ($\lambda_{spp}/L_{spp} = 2.5$) and therefore the propagation length is less than the SPP wavelength (Fig. 4).

3. Nanocavity

At the first sight, a strong absorption in the metal prevents us to design a device based on extremely slow SPPs. Can we nevertheless use such modes? Consider the energy flux in the IMI guide (Fig. 5). We will take the small region of the waveguide between x and $x + \Delta x$.

$$\int_{-\infty}^{+\infty} W(x,z,t)\mathrm{d}z = \frac{1}{32\pi k^2}|H_{\mathrm{low}}(x,t)|^2 \left\{\frac{|\kappa_3|^2 + |\beta|^2 + k^2\varepsilon_3}{\varepsilon_3 \mathrm{Re}\kappa_3} + \frac{(|\kappa_2|^2 + |\beta|^2 + k^2\varepsilon_2)\varepsilon_2}{\varepsilon_3^2 \mathrm{Re}\kappa_2}\frac{|\gamma_{3+}|^2}{|\gamma_{2-}|^2} + \frac{|\gamma_{3+}|^2 + |\gamma_{3-}|^2}{2|\kappa_1|^2\varepsilon_3^2} + \frac{\left[(2\varepsilon_r - \mathrm{Re}\varepsilon_1)(|\kappa_1|^2 + |\beta|^2) + k^2|\varepsilon_1|^2\right](|\gamma_{3+}|^2 + |\gamma_{3-}|^2)}{2|\kappa_1|^2\varepsilon_3^2|\varepsilon_1|^2}\frac{\sinh(\mathrm{Re}\kappa_1 d)}{\mathrm{Re}\kappa_1} + \frac{\left[(2\varepsilon_r - \mathrm{Re}\varepsilon_1)(|\beta|^2 - |\kappa_1|^2) + k^2|\varepsilon_1|^2\right](\gamma_{3+}\gamma_{3-}^* + \gamma_{3+}^*\gamma_{3-})}{2|\kappa_1|^2\varepsilon_3^2|\varepsilon_1|^2}\frac{\sin(\mathrm{Im}\kappa_1 d)}{\mathrm{Im}\kappa_1}\right\}, \quad (4)$$

where quantity $H_{\mathrm{low}}(x,t)$ has the meaning of the complex amplitude of the magnetic field at the lower interface of the film ($z = -d/2$), $\kappa_i = \sqrt{\beta^2 - (\omega/c)^2\varepsilon_i}$ ($i = 1,2,3$) are penetration constants and notation $\gamma_{i\pm} = (\kappa_1\varepsilon_i \pm \kappa_i\varepsilon_1 \exp(\pm\kappa_1 a))$ ($i = 2,3$) is used for the sake of brevity.

In the stationary regime ($I(x,t) = I(x)$), the time-average density of the energy and the Joule loss power are time-independent ($W(x,t) = W(x)$, $J(x,t) = J(x)$), therefore $I(x) - I(x + \Delta x) \approx J(x + \Delta x/2)\Delta x$, or more precisely:

$$\mathrm{grad}\, I(x) = -J(x) \quad (5)$$

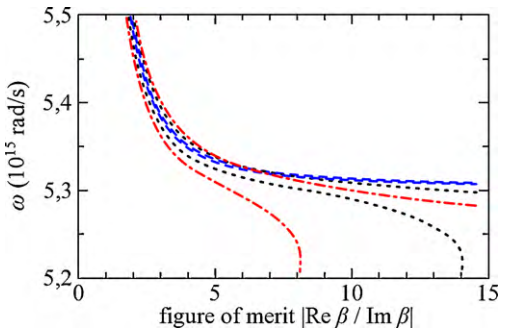

Fig. 3. Figure of merit for the SPP in the Al_2O_3–Ag-ZrO_2 guide for different values of the metal damping constant: $\Gamma = 7 \times 10^{13}$ rad s^{-1} (dash-dotted red line), $\Gamma = 4 \times 10^{13}$ rad s^{-1} (dotted black line) and $\Gamma = 7 \times 10^{12}$ rad s^{-1} (dashed blue line). The core thickness $d = 15$ nm. (For interpretation of the references to color in this figure legend, the reader is referred to the web version of the article.)

Taking into account Eq. (1), we get:

$$\frac{\mathrm{d}}{\mathrm{d}x}\int W(x,z)\mathrm{d}z = -\frac{1}{\upsilon_{\mathrm{E}}}J(x) \tag{6}$$

Eq. (6) is a differential equation that describes the way the amplitude of the guided mode changes with the distance. Since the energy velocity is very small and Joule losses are large.

$$J(x,t) = \frac{\Gamma\omega_{\mathrm{p}}^2}{32\pi(\omega^2+\Gamma^2)}|H_{\mathrm{low}}(x,t)|^2 \times \left\{\frac{|\beta|^2+|\kappa_1|^2}{k^2|\varepsilon_1|^2}\frac{|\gamma_{3+}|^2+|\gamma_{3-}|^2}{|\kappa_1|^2\varepsilon_3^2}\frac{\sinh(\mathrm{Re}\kappa_1 d)}{\mathrm{Re}\kappa_1} + \frac{|\beta|^2-|\kappa_1|^2}{k^2|\varepsilon_1|^2}\frac{\gamma_{3+}\gamma_{3-}^*+\gamma_{3-}\gamma_{3+}^*}{|\kappa_1|^2\varepsilon_3^2}\frac{\sin(\mathrm{Im}\kappa_1 d)}{\mathrm{Im}\kappa_1}\right\}, \tag{7}$$

the intensity decreases rapidly with the distance.

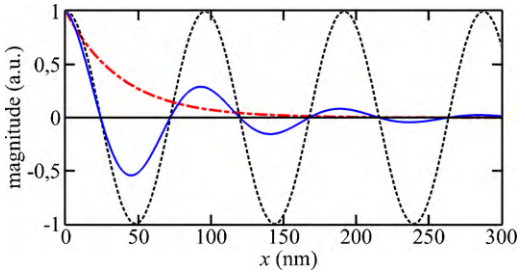

Fig. 4. Spatial distribution of the intensity (dash-dotted red line) and the magnitude of the electric field of the SPP at fixed time (solid blue line) along the Al_2O_3–Ag-ZrO_2 guide ($\Gamma = 7 \times 10^{13}$ rad s^{-1}, $\omega = 5.305 \times 10^{15}$ rad s^{-1}). Also shown is the distribution of the electric field magnitude at fixed time in the lossless cases (dotted black line). (For interpretation of the references to color in this figure legend, the reader is referred to the web version of the article.)

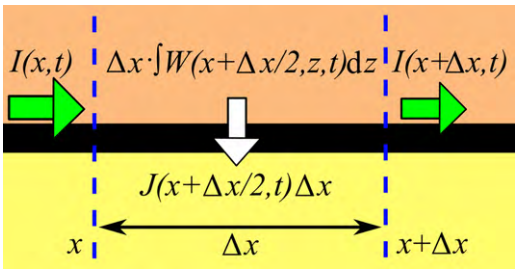

Fig. 5. Schematic diagram of the energy flux and the absorption of energy in the IMI guide. $I(x,t)$ and $I(x+\Delta x,t)$ are the time-average total power flow at x and $x+\Delta x$, $J(x,t)$ is the Joule loss power per unit guide length and $W(x,t)$ is the time-average energy density.

Somewhat significantly different can be found when we deal with transient processes. Now the Joule loss term, energy density and total power flow depend on t and we can write:

$$\begin{aligned}&\Delta x\int W\left(x+\frac{\Delta x}{2},z,t+\Delta t\right)dz - \Delta x\int W\left(x+\frac{\Delta x}{2},z,t\right)dz \\ &\approx -\left[I\left(x+\Delta x,t+\frac{\Delta t}{2}\right)-I\left(x,t+\frac{\Delta t}{2}\right)\right]\Delta t - J\left(x+\frac{\Delta x}{2},t+\frac{\Delta x}{2}\right)\Delta x\Delta t\end{aligned}$$

Letting Δx tend to zero and taking into consideration Eq. (1), we obtain:

$$\frac{\partial}{\partial t}\int W(x,z,t)dz = -\upsilon_{\mathrm{E}}\frac{\partial}{\partial x}\int W(x,z,t)dz - J(x,t) \tag{8}$$

One can easily see that, if the energy velocity or the gradient of the time-average energy per unit guide length is small, the first term in the right-hand part of Eq. (8) becomes much less than the second one and the only way for the energy to dissipate is the Joule heating:

$$\frac{\partial}{\partial t}\int W(x,z,t)dz \approx -J(x,t) \tag{9}$$

It should be noted that for the infinite film it is not necessary for υ_{E} and $\partial W(x,z,t)/\partial x$ to be equal to zero simultaneously. For instance, if $\partial W(x,z,t)/\partial x \approx 0$ and $\upsilon_{\mathrm{E}} \sim c$, the energy flows along the guide with the speed of about c but the first term in Eq. (8) is approximately zero. In this case, if the SPP impinges on the edge of the film, it is mostly scattered out as photons and loses almost all its energy, since the reflectivity coefficient r is

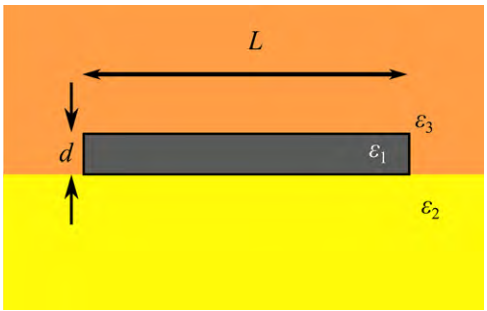

Fig. 6. Sketch of the cavity based on the IMI guide of finite length L.

much less than 1 [26]. The scattering loss power is about $(1-2r)\upsilon_E \int W(x_{edge}, z, t)dz$, where x_{edge} is the x-coordinate of the edge of the film. So, we should take into account this type of losses because all devices are finite and, moreover, they ought to be tiny. To minimize scattering losses at the edge of the film, it is necessary to decrease the energy velocity.

Also, there are other types of losses: a leakage radiation due to coupling to other waveguides and a leakage radiation due to a surface roughness. The first kind of losses depends highly on the certain configuration and will not be analyzed here and the second one can be decreased and becomes much less than the Joule loss term.

Finally, we have considered all types of losses and can conclude: if the energy velocity is close to zero, losses are determined mainly by the Joule heating even though the film length L is sufficiently small. So, now we can propose a cavity based on the IMI guide of finite length [27] (Fig. 6). Such a cavity does not require any resonator grids owing to the fact that the energy velocity is exceedingly small and thus Joule loss term, which slightly depends on the cavity geometry, is much greater than other loss terms.

The quality factor is defined as follows:

$$Q = 2\pi \frac{\int_{-\infty}^{+\infty} W dz}{(2\pi/\omega)(J + R_E + R_L)}, \tag{10}$$

where the denominator is the energy dissipated in one cycle, R_E is the radiation loss power associated with the edge scattering losses due to the nonzero energy velocity and R_L is the leakage radiation into surrounding media due to the roughness and coupling to other waveguides. According to Eq. (10), in the relaxation process the total energy stored in the cavity (U) depends on time as $U(t) = U(0)\exp(-\omega t/Q)$. An analytical estimation of Q can be obtained, we should only evaluate R_L and R_E because the other terms are already known (Eqs. (4) and (7)). In our estimations, we will use the simplest approximation of the quality factor assuming R_L to be zero. As for R_E, it has the meaning of the ratio of the edge scattering loss power P to the length of the cavity L:

$$R_E = \frac{P}{L} = \upsilon_E \int_{-\infty}^{+\infty} W(x_0, z, t) \frac{dz}{L_{eff}}. \tag{11}$$

Here, x_0 is the certain point of the cavity and L_{eff} is the effective length of the cavity, i.e. the length of the cavity, which has the zero reflectivity coefficient ($r = 0$) and a uniform distribution of the energy along the waveguide core ($\int W(x, z, t)dz = \int W(z, t)dz$) but the same quality factor Q as the cavity under investigation. A clear analytical expression for L_{eff} is complicated, since L_{eff} depends on parameters of the cavity, on x_0 and on the angular frequency, nevertheless we can easily get a good approach. As was mentioned in Section 2, the edge scattering loss power is proportional to the total power flow and is evaluated as $P \approx (1-2r)\upsilon_E \int W(x_{edge}, z, t)dz \approx (1-r)\upsilon_E \int W(x_0, z, t)dz$, if x_0 lies away from the cavity edges. Consequently, according to Eq. (11), we get:

$$L_{eff} = \frac{L}{1-r} \tag{12}$$

To give an example, we have estimated the quality factor of the Al_2O_3–Ag-ZrO_2 waveguide of finite thickness (d = 15 nm, L_{eff} = 160 nm) at the frequency of ZGV ($\omega = 5.305 \times 10^{15}$ rad s^{-1}) and have found Q to be equal to 66 for the backward wave mode and 58 for the forward wave mode. To increase Q, one should decrease the energy velocity (increase the frequency) or decrease the damping constant of the metal (Table 1). Unfortunately, it is difficult to decrease the energy velocity appreciably, because at small values of υ_E the imaginary part of β is sufficiently large (Fig. 2(b)) and hence such modes become relatively difficult to excite. As for decreasing of Γ, there are many problems in this way. However, at least two promising techniques, that do not require low temperatures and other specific conditions, exist. The first of them is alloying a noble metal with another metal [28] and the second is a compensation of losses with the help of an ''active'' medium [29].

Table 1
Quality factor of the Al_2O_3–Ag-ZrO_2 nanocavity for different parameters (the damping constant, the operating frequency and the mode excited), $d = 15$ nm, $L_{eff} = 160$ nm.

	Q-factor					
	$\Gamma = 7 \times 10^{13}$ rad s^{-1}		$\Gamma = 4 \times 10^{13}$ rad s^{-1}		$\Gamma = 7 \times 10^{12}$ rad s^{-1}	
	$\omega = 5.31 \times 10^{15}$ rad s^{-1}	$\omega = 5.4 \times 10^{15}$ rad s^{-1}	$\omega = 5.31 \times 10^{15}$ rad s^{-1}	$\omega = 5.4 \times 10^{15}$ rad s^{-1}	$\omega = 5.31 \times 10^{15}$ rad s^{-1}	$\omega = 5.4 \times 10^{15}$ rad s^{-1}
Forward wave mode	61	75	101	132	510	760
Backward wave mode	67	76	110	132	530	760

4. Estimation of the quality factor

The dispersion equation for the SPP guided by the IMI structure [7,8,14] is difficult to solve, since the angular frequency ω and the wavevector β may be both complex. Nevertheless, there are two commonly used simplifications: to consider a complex β and a real ω [19,24,25] and, alternatively, a complex ω and a real β [25,30]. None of them gives the exact solution in our case. In this paper, we have discussed in details the case when β is complex and ω is real. This approach is almost ideal for stationary (time-independent) regime and is suited for the description of the wave propagation and energy transfer. When ω is complex and β is real, the dispersion curves in this case (Fig. 7) differ highly from Fig. 2(a) and (b). Two curves for $\Gamma = 0$ and for $\Gamma = 7 \times 10^{13}$ rad s^{-1} almost completely coincide (Fig. 7), however the group velocity can not be used as the measure of the energy transport [25], though it is almost zero at some points. This approach is suited for the analysis of time-dependent processes [30] but it does not convenient for the description of energy transport. Since the energy velocity does not achieve zero [19,24,25], the scattering losses at the edge of the cavity should be taken into account (Section 3) and therefore R_E must be estimated. But if the length of the cavity is much greater than λ_{spp}, L_{spp} and $\upsilon_E \cdot Q/\omega$, we can neglect R_E with respect to the Joule loss term J (Eq. (10)). In that case, $Q = Q_\infty \approx -\mathrm{Re}(\omega)/\mathrm{Im}(2\omega)$. For example, $\mathrm{Re}(\omega) = 5.304 \times 10^{15}$ rad s^{-1}, $\mathrm{Im}(\omega) = -3.12 \times 10^{13}$ rad s^{-1} and we get $Q_\infty \approx 85$. If one considers a finite cavity (L is finite), then R_E must be calculated. Eqs. (7) and (11) are derived in the complex-β approach, however, we will use them for comparison of two different approaches. Eqs. (7) and (11) give $R_E/J = 0.25$ (backward wave mode) and $R_E/J = 0.55$ (forward wave mode) for the cavity with $L_{eff} = 160$ nm. Finally, we have $Q = Q_\infty/(1 + R_E/J)$: $Q \approx 55$ (forward wave mode) and $Q \approx 68$ (backward wave mode). For the same frequency ($\omega = 5.304 \times 10^{15}$ rad s^{-1}) the complex-β approach gives $Q = 58$ (forward wave mode) and $Q = 66$ (backward wave mode). This example shows that the Joule losses calculated using the complex-β approach and the complex-ω approach are identical. A more rigorous

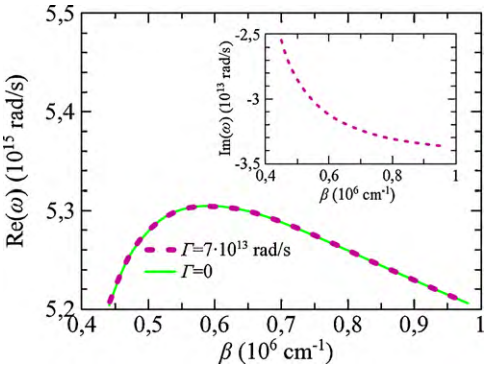

Fig. 7. Dispersion curves of the SPP in the Al_2O_3–Ag-ZrO_2 waveguide structure ($d = 15$ nm) using the complex-ω approach: $\mathrm{Re}(\omega)$ versus β in the figure and $\mathrm{Im}(\omega)$ versus β in the inset, only the antisymmetric mode is shown.

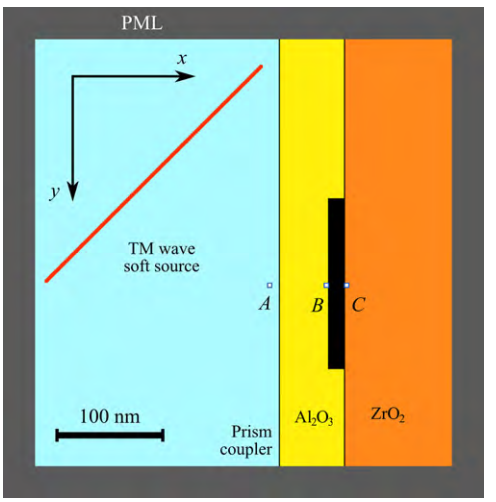

Fig. 8. The simulation geometry, A, B and C are points, at which we record field magnitudes. Red line is the soft source [33]. The source radiates a two-dimensional TM wave with a Gaussian amplitude distribution. (For interpretation of the references to color in this figure legend, the reader is referred to the web version of the article.)

consideration and comparison of the above approaches in the vicinity of the ZGV point is under work and will be presented elsewhere.

5. Stored light in the nanocavity

We have shown that it is possible to design a cavity with a sufficiently high quality factor and extremely small size (with all dimensions less than the wavelength of light). In this section, we demonstrate a stored light in such a plasmonic cavity. An ultra-short light pulse excites the cavity. There is a number of ways to couple light to the SPP owing to the simple shape of the cavity and its planar geometry. In this work, the ordinary prism coupler is used for the sake of simplicity. After the cavity is excited, it stores the energy of the electromagnetic wave for a long time (much greater than the pulse duration) due to a high Q-factor. We have used our 2D finite difference time domain (FDTD) code and have carried out simulations with the pulse duration of 8 fs at the central frequency of 845 THz (that corresponds to the wavelength of light in vacuum of 355 nm). Such a frequency is chosen by the reason of a high tunability of the cavity. One is able to change the operating frequency from 750 to 1000 THz by means of variation of permittivities of the insulator media. The upper limit corresponds to the frequency of the cerium laser, where cerium is used as a dopant in the crystal Ce:LiCaF [31]. In principle, such a laser is able to support 3 fs pulses. The lower limit is the second harmonic of the Ti:Sapphire laser whose pulse duration is less than 5 fs [32]. Thus we have taken 845 THz (355 nm) as an average value. The simulation geometry is depicted in Fig. 8, it consists of a 60 nm layer of Al_2O_3, 15 nm layer of silver, 100 nm layer of ZrO_2 right after, and 230 nm thick prism coupler on the left of the cavity. The length of the metal strip equals 160 nm. A 30 nm perfectly matched layer (PML) [34] surrounds the computational space.

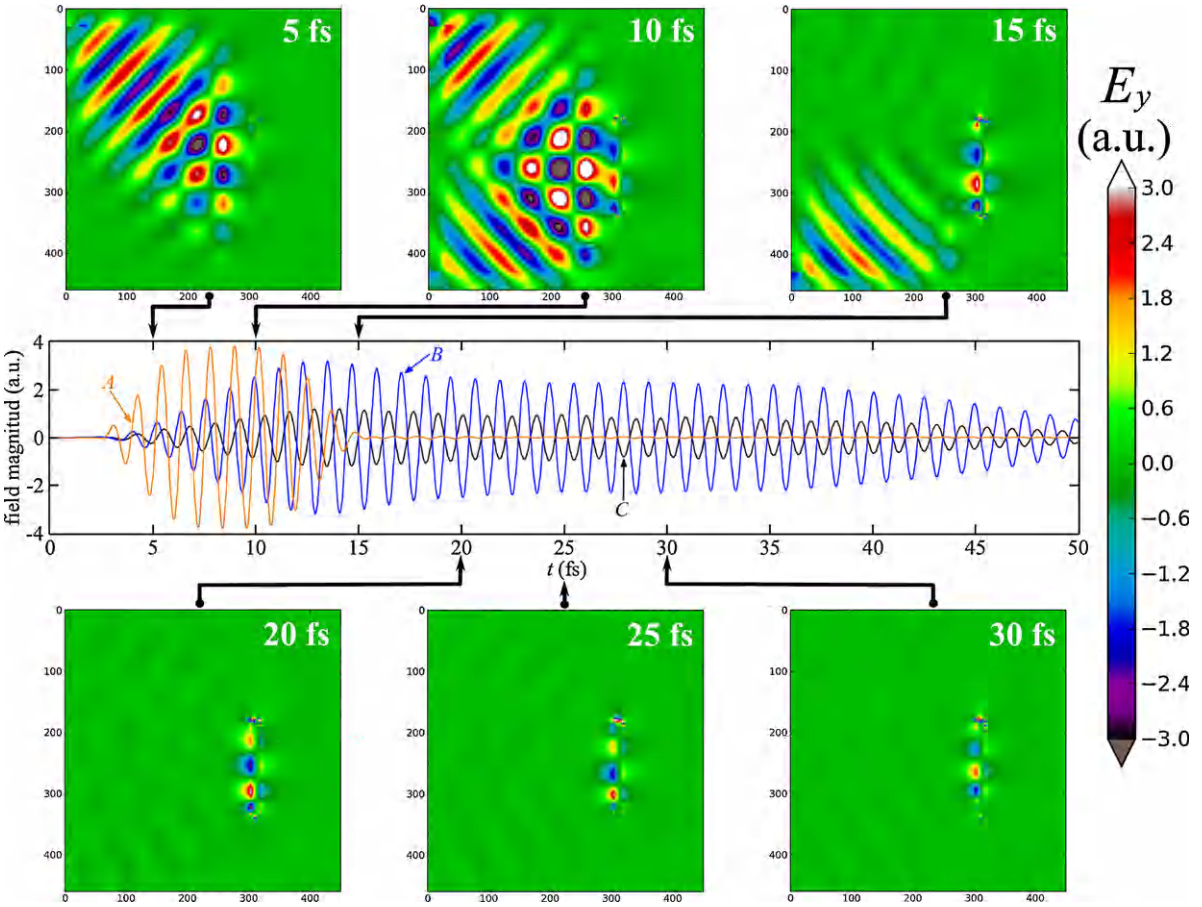

Fig. 9. The longitudinal electric field (E_y) distribution at different moments of time and the time dependence of E_y (the field at the point A – orange line, at the point B – blue line, at the point C – black line). (For interpretation of the references to color in this figure legend, the reader is referred to the web version of the article.)

The component of the wavevector of the incident light parallel to the layer interfaces is equal to $6.55 \times 10^5\ \mathrm{cm}^{-1}$, thereby the backward wave mode of the IMI guide is mainly excited (Fig. 2(a) and (b)). After reflecting from the prism-Al_2O_3 interface, the light pulse leaves the simulation region, however the energy of light that has been transformed into the SPP keeps on storing. Fig. 9 shows the time dependence of the longitudinal electric field (the component parallel to the layer interfaces, E_y) taken at three points (A, B and C) and the spatial distribution of E_y at different moments of time. Point A is far away from the cavity and gives information about the exciting light pulse, points B and C lie at different boundaries of the IMI guide core and thus show the essence of the transient process. The relative phase of the field at the point B and the field at C equals π, since the antisymmetric mode is excited. After excitation (t = 3–13 fs Fig. 9), the amplitude of the electric field in the cavity begins slowly decreasing but after $t \approx 43$ fs (about 30 fs after exciting) the rate of decay increases dramatically (Fig. 9). This feature of such a cavity can be easily explained: the energy velocity of the SPP is about $-2.5 \times 10^6\ \mathrm{m\ s}^{-1}$ (Fig. 2(c)), points B and C are placed at a distance of 80 nm from the edges of the cavity thus $8 \times 10^{-8}\ \mathrm{m}/2.5 \times 10^6\ \mathrm{m\ s}^{-1} = 32$ fs. The energy flows upward along the waveguide core (the backward wave mode is excited) with the speed υ_E. At the initial time ($t \approx 13$ fs) the SPP occupies the entire volume of the cavity (the full length L) but after $t \approx 45$ fs it occupies only about a half of the cavity, i.e. the energy of the SPP is mostly localized between the point C and the upper edge of the cavity. Therefore, the effective length of the cavity is time-dependent. It decreases with time:

$$L_{\mathrm{eff}} = L_{\mathrm{eff}}(t) \approx L_{\mathrm{eff}}(0)\frac{[L - |\upsilon_E|t]}{L} \approx (1 - r)(L - |\upsilon_E|t), \quad (13)$$

consequently, the quality factor is time-dependent too: $Q = Q(L_{\mathrm{eff}}(t)) = Q(t)$ (Eqs. (10) and (11)). We obtain that $U(t) = U(0)\exp(-\omega t/Q(t))$, in other words the total energy stored in the cavity does not depend exponentially on time, it decays faster than the simple exponential decay function $U(t) = U(0)\exp(-\omega t/Q(0))$. Fortunately, our estimations demonstrate that $R_E/J = 0.24$ for $L_{\mathrm{eff}} = 160$ nm and $R_E/J = 0.46$ for $L_{\mathrm{eff}} = 80$ nm, that is why $Q(L_{\mathrm{eff}} = 80\ \mathrm{nm}) \approx 0.85 \times Q(L_{\mathrm{eff}} = 160\ \mathrm{nm})$, i.e. Q depends slightly on the effective length of the cavity, therefore Q depends slightly on t and $U(t) \approx U(0)\exp(-\omega t/Q(0))$.

6. Conclusion

In conclusion, we have studied extremely slow SPPs guided by the IMI guide whose energy velocities are close to zero and have obtained that the energy velocity can be less than 1/100 c. It was shown that for such SPPs the IMI guide of finite length can be a cavity with a high Q-factor. We have theoretically estimated Q and numerically demonstrated a possibility to store light by means of transformation into the slow SPP guided by the IMI guide. The storage time equals 10–200 fs and depends on the damping in the metal film and the length of the cavity. In addition, the cavity is easily fabricated due to its planar geometry and three layer structure. The nanocavity obtained in this work could be utilized in many fields of optical science and engineering, as example, detection of ultra-short and few-cycle pulses in ultraviolet and design of optical memory.

Acknowledgments

The authors thank the team of the Laboratory of Nanooptics and Femtosecond Electronics, Department of General Physics, for their assistance. This work was supported in part by the Russian Foundation for Basic Research (grants no. 09-07-12144-ofi-m and 09-07-00285) and the Russian Federal Agency of Education (grants no. 2.1.1/236, 2.1.1/523 and P513).

References

[1] K.L. Tsakmakidis, A.D. Boardman, O. Hess, Nature 450 (2007) 397.
[2] Qiang Bai, Jing Chen, Nian-Hai Shen, Chen Cheng, Hui-Tian Wang, Opt. Express 18 (2010) 2106.
[3] H. Gersen, T.J. Karle, R.J.P. Engelen, W. Bogaerts, J.P. Korterik, N.F. van Hulst, T.F. Krauss, L. Kuipers, Phys. Rev. Lett. 94 (2005) 073903.
[4] S.I. Bozhevolnyi (Ed.), Plasmonic Nanoguides and Circuits, Pan Stanfod Publishing, Singapore, 2009.
[5] S.I. Bozhevolnyi, V.S. Volkov, E. Devaux, J. Laluet, T.W. Ebbesen, Nature 440 (2006) 508.
[6] V.M. Shalaev, S. Kawata (Eds.), Nanophotonics with Surface Plasmons, Elsevier, The Netherlands, 2007.
[7] V.M. Agranovich, D.L. Mills (Eds.), Surface Polaritons, North-Holland Publishing Company, Amsterdam, 1982.
[8] A.V. Zayats, I.I. Smolyaninov, A.A. Maradudin, Phys. Rep. 408 (2005) 131.
[9] I.I. Smolyaninov, J. Opt. A: Pure Appl. Opt. 7 (2005) S165.
[10] I.I. Smolyaninov, New J. Phys. 10 (2008) 115033.
[11] V. Mikhailov, G.A. Wurtz, J. Elliott, P. Bayvel, A.V. Zayats, Phys. Rev. Lett. 99 (2007) 083901.
[12] W.P. Allis, S.J. Buchsbaum, A. Bers, Waves in Anisotropic Plasma, M.I.T. Press, Cambridge, 1963.
[13] K.L. Kliewer, R. Fuchs, Phys. Rev. 153 (1967) 498.

[14] E.N. Economou, Phys. Rev. 182 (1969) 539.
[15] D.Yu. Fedyanin, A.V. Arsenin, V.G. Leiman, A.D. Gladun, Quantum Electron. 39 (8) (2009) 745.
[16] A. Karalis, E. Lidorikis, M. Ibanescu, J.D. Joannopoulos, M. Soljačić, Phys. Rev. Lett. 95 (2005) 063901.
[17] M.I. Stockman, Phys. Rev. Lett. 98 (2007) 177404.
[18] J.A. Dionne, E. Verhagen, A. Polman, H.A. Atwater, Opt. Express 16 (2008) 19001.
[19] D.Yu. Fedyanin, A.V. Arsenin, V.G. Leiman, A.D. Gladun, J. Opt. 12 (2010) 015002.
[20] P.B. Johnson, R.W. Christy, Phys. Rev. B 6 (1972) 4370.
[21] H. Kogelnik, in: T. Tamir (Ed.), Theory of Dielectric Waveguides in Integrated Optics, Springer, Berlin, 1979.
[22] V.V. Shevchenko, Physics–Uspekhi 50 (3) (2007) 301.
[23] P. Milloni, Fast Light, Slow Light and Left-Handed Light, Institute of Physics, Bristol, 2005.
[24] A. Reza, M.M. Dignam, S. Hughes, Nature London 455 (2008) E10.
[25] C. Peijun Yao, A. Van Vlack, M. Reza, M.M. Patterson, S. Dignam, Hughes, Phys. Rev. B 80 (2009) 195106.
[26] R. Gordon, Phys. Rev. B 74 (2006) 153417;
R. Gordon, Phys. Rev. B 75 (2007) 039901(E).
[27] D.Yu. Fedyanin, A.V. Arsenin, AIP Conf. Proc. 1176 (2009) 108.
[28] D.A. Bobb, G. Zhu, M. Mayy, A.V. Gavrilenko, P. Mead, V.I. Gavrilenko, M.A. Noginov, Appl. Phys. Lett. 95 (2009) 151102.
[29] G. Zhu, M. Mayy, M. Bahoura, B.A. Ritzo, H.V. Gavrilenko, V.I. Gavrilenko, M.A. Noginov, Opt. Express 16 (2008) 15576.
[30] A. Karalis, J.D. Joannopoulos, M. Soljacic, Phys. Rev. Lett. 103 (2009) 043906.
[31] E. Granados, D.W. Coutts, D.J. Spence, Opt. Lett. 34 (2009) 1660.
[32] U. Keller, Nature 424 (2003) 831.
[33] A. Taflove, S.C. Hagness, Computational Electrodynamics: The Finite-Difference Time-Domain Method, 2nd ed., Artech House, Boston, 2005.
[34] J.P. Berenger, Perfectly Matched Layer (PML) for Computational Electromagnetic, Morgan and Claypool, San Rafael, 2007